

# DRAINED RESIDUAL STRENGTH OF COHESIVE SOILS

By Timothy D. Stark,<sup>1</sup> Associate Member, ASCE,  
and Hisham T. Eid,<sup>2</sup> Student Member, ASCE

**ABSTRACT:** Results of torsional ring shear tests on cohesive soils reveal that the drained residual strength is related to the type of clay mineral and quantity of clay-size particles. The liquid limit is used as an indicator of clay mineralogy, and the clay-size fraction indicates quantity of particles smaller than 0.002 mm. Therefore, increasing the liquid limit and clay-size fraction decreases the drained residual strength. The ring shear tests also reveal that the drained residual failure envelope is nonlinear, and the nonlinearity is significant for cohesive soils with a clay-size fraction greater than 50% and a liquid limit between 60% and 220%. This nonlinearity should be incorporated into stability analyses. An empirical correlation for residual friction angle is described that is a function of liquid limit, clay-size fraction, and effective normal stress. Previous residual strength correlations are based on only one soil index property and provide a residual friction angle that is independent of effective normal stress. For slope stability analyses, it is recommended that the residual strength be modeled using the entire nonlinear residual strength envelope or a residual friction angle that corresponds to the average effective normal stress on the slip surface.

## INTRODUCTION

The drained residual shear strength of cohesive soils is a crucial parameter in evaluating the stability of preexisting slip surfaces in new and existing slopes and the design of remedial measures. At present, the reversal direct shear test is widely used to measure the drained residual strength of clays and clayshales even though it has several limitations. The primary limitation is that the soil is sheared forward and then backward until a minimum shear resistance is measured. Each reversal of the shear box results in a horizontal displacement that is usually less than 0.5 cm. As a result, the specimen is not subjected to continuous shear deformation in one direction, and thus a full orientation of the clay particles parallel to the direction of shear may not be obtained.

The main advantage of the torsional ring shear apparatus is that it shears the specimen continuously in one direction for any magnitude of displacement. This allows clay particles to be oriented parallel to the direction of shear and a residual strength condition to develop. Other advantages of the ring shear apparatus include a constant cross-sectional area of the shear surface during shear, minimal laboratory supervision during shear, and the possible use of data acquisition techniques.

The results of torsional ring shear tests on 32 clays and shales revealed that the drained residual failure envelope is nonlinear. The 32 clays and clayshales are listed in Table 1 by increasing liquid limit. This stress-dependent behavior of the drained residual failure envelope has also been observed by a number of other researchers, including Kenney (1967), Lupini

---

<sup>1</sup>Asst. Prof. of Civ. Engrg., Univ. of Illinois, Newmark Civ. Engrg. Lab. MC-250, 205 N. Mathews Ave., Urbana, IL 61801-2352.

<sup>2</sup>Grad. Res. Asst. of Civ. Engrg., Univ. of Illinois, Urbana, IL 61801.

Note. Discussion open until October 1, 1994. To extend the closing date one month, a written request must be filed with the ASCE Manager of Journals. The manuscript for this paper was submitted for review and possible publication on November 13, 1990. This paper is part of the *Journal of Geotechnical Engineering*, Vol. 120, No. 5, May, 1994. OASCE, ISSN 0733-9410/94/0005-0856/\$2.00 + \$.25 per page. Paper No. 909.

**TABLE 1. Clay and Shale Samples Used in Ring Shear Tests**

Soil number (1)	Clay and shale samples (2)	Clay and shale locations (3)	Initial water content (%) (4)	Specific unit weight (kN/m <sup>3</sup> ) (5)	Liquid limit (6)	Plastic limit (7)	Clay-size fraction (%) (8)	Activity (PIICF) (9)
1	Glacial Till	Urbana, Ill.	8.4	16.1	24	16	18	0.44
2	Loess	Vicksburg, Miss.	14.0	16.5	28	18	10	1.00
3	Bootlegger Cove clay	Anchorage, Alaska	34.8	18.6	35	18	44	0.39
4	Duck Creek shale <sup>1</sup>	Fulton, Ill.	5.3	24.0	37	25	19	0.63
5	Chinle (red) shale <sup>a</sup>	Holbrook, Ariz.	10.9	22.7	39	20	43	0.44
6	Colorado shalc <sup>1</sup>	Montana, Mont.	5.6	21.2	46	25	73	0.29
7	Panoche mudstone	San Francisco, Calif.	14.2	19.6	47	27	41	0.49
8	Four Fathom shale <sup>a</sup>	Durham, England	3.3	25.1	50	24	33	0.79
9	Mancos shale	Price, Utah	4.9	24.5	52	20	63	0.51
10	Panoche shalc	San Francisco, Calif.	12.0	20.2	53	29	50	0.48
11	Comanche shalc <sup>a</sup>	Proctor Dam, Tcx.	11.5	23.1	62	32	68	0.44
12	Bearpaw shale. <sup>1</sup>	Billings, Mont.	15.7	21.8	68	24	51	0.86
13	Slide debris	San Francisco, Calif.	18.1	19.6	69	22	56	0.84
14	Bay mud	San Francisco, Calif.	73.0	15.0	76	41	16	2.19
15	Patapsco shalc <sup>1</sup>	Washington, D.C.	21.6	20.7	77	25	59	0.88
16	Pierre shale. <sup>1</sup>	Limon, Colo.	24.3	20.1	82	30	42	1.24
17	Santiago claystone	San Diego, Calif.	20.7	19.6	89	44	57	0.79
18	Lower Pepper shale	Waco Dam, Tex.	21.0	20.3	94	26	77	0.88
19	Altamira bentonitic tuff	Portuguese Bend, Calif.	62.0	17.5	98	37	68	0.90
20	Brown London clay	Bradwell, England	33.0	18.9	101	35	66	1.00
21	Cucaracha shale <sup>1</sup>	Panama Canal	18.4	20.7	111	42	63	1.10
22	Otay bentonitic shalc	San Diego, Calif.	27.0	17.6	112	53	73	0.81
23	Denver shale. <sup>1</sup>	Denver, Colo.	30.5	18.7	121	37	67	1.25
24	Bearpaw shalc <sup>1</sup>	Saskatchewan, Canada	27.3	19.0	128	27	43	2.35
25	Oahe firm shalc	Oahe Dam, S.Dak.	27.6	20.1	138	41	78	1.24
26	Claggett shalc <sup>a</sup>	Benton, Mont.	11.7	22.7	157	31	71	1.78
27	Taylor shale <sup>1</sup>	San Antonio, Tcx.	35.2	18.0	170	39	72	1.82
28	Pierre shale <sup>a</sup>	Reliance, S.Dak.	42.8	17.7	184	55	84	1.54
29	Oahe bentonitic shalc	Oahe Dam, S.Dak.	35.4	18.9	192	47	65	2.23
30	Panoche clay gouge	San Francisco, Calif.	34.8	21.8	219	56	72	2.26
31	Lea Park bentonitic shalc	Saskatchewan, Canada	36.0	17.3	253	48	65	3.15
32	Bearpaw shalc <sup>a</sup>	Ft. Peck Dam, Mont.	15.8	21.8	288	44	88	2.77

<sup>a</sup>Index properties from Mccrri and Cepeda-Diaz (1086).

et al. (1981), Bromhead and Curtis (1983), Hawkins and Privett (1984; 1985), Lambe (1985), Skempton (1985), Anayi et al. (1988; 1989), and Maksimovic (1989). Therefore, a disadvantage of existing drained residual strength correlations is that a single value of drained residual friction angle does not accurately model the nonlinear residual failure envelope. The main objectives of this study were to gain an understanding of the nonlinearity of the drained residual failure envelope, investigate the importance of the nonlinearity in stability analyses, and develop a new correlation that describes the nonlinear residual failure envelope.

## SOIL DESCRIPTION AND TEST PROCEDURE

A modified Bromhead ring shear apparatus (Stark and Eid 1993) was used for testing the 32 clays and clayshales. The original ring shear apparatus is described by Bromhead (1979). The ring shear specimen is annular with an inside diameter of 7 cm and an outside diameter of 10 cm. Drainage is provided by annular bronze porous stones secured to the bottom of the specimen container and to the loading platen. The specimen is confined radially by the specimen container, which is 0.5 cm deep.

The specimen preparation procedure for the ring shear apparatus was adapted from that used by Mesri and Cepeda-Diaz (1986) for the direct shear apparatus. Remolded shale specimens are obtained by air drying a representative sample of each shale. The air-dried shale is ball-milled until all of the representative sample passes the U.S. Standard sieve #200. Remolded silt and clay specimens (soil numbers 1, 2, 3, 13, and 14 in Table 1) are obtained by air drying a representative sample, crushing it with a mortar and pestle, and processing it through the #40 sieve. Ball-milling is not used for these specimens, because it would change the texture and gradation of the soil. In both cases, distilled water is added to the processed soil until a liquidity index of about 1.5 is obtained. The sample is then allowed to rehydrate for at least one week in a moist room. A spatula is used to place the remolded soil paste into the annular specimen container. The top of the specimen is planed flush with the top of the specimen container using a 15.2-cm-long surgical razor blade. It should be noted that the liquid limit, plastic limit, and clay size fraction of the specimens were measured using the ball-milled or sieved soil samples.

The modified Bromhead ring shear apparatus allows a remolded specimen to be overconsolidated and precut, which simulates the field conditions that lead to the development of a residual strength condition in overconsolidated clays and clayshales. A consolidation stress of 700 kPa was chosen to represent the maximum effective stress that could be encountered in slope and embankment field case histories. The specimens were sheared at effective normal stresses between 50 and 700 kPa or an overconsolidation ratio of 14 to 1, respectively.

The specimen is precut prior to shear by exposing the top of the specimen after consolidation at 700 kPa. The specimen is exposed by lowering the outer ring and inner core that surround the annular specimen. The inner core of the annular specimen container is lowered by threading it out of the bottom of the specimen container such that the top of the core is approximately 0.05 cm below the top surface of the specimen. The specimen container is then placed on a horizontal surface and the outer ring is pushed down until it becomes flush with the horizontal surface and center core. The lowering of the center core and outer ring exposes approximately 0.05 cm of the annular specimen above the top of the container.

A shear surface is created in the overconsolidated soil by slowly rotating the top platen in the direction of shear. This also allows the top platen and porous stone to be separated from the specimen container. A 15.2-cm-long surgical razor blade is used to precut the exposed specimen. The razor blade is placed on the upper surface of the specimen container and moved in the direction of shear until a smooth and polished surface is obtained. Therefore, the precut specimen is flush with the top surface of the specimen container prior to shearing. When the top platen separated from the specimen container, a layer of soil 0.01–0.03 cm thick remains attached to the knurled porous stone. This soil was previously presheared and usually exhibit; a smooth surface.

After precutting, the top platen and specimen container are reassembled and loaded to an effective normal stress of 50 or 60 kPa. All ring shear specimens were sheared at a drained displacement rate of 0.018 mm/min. This displacement rate is based on values of coefficient of consolidation evaluated from oedometer tests and during consolidation of the ring shear specimen to 700 kPa. The procedure described by Gibson and Henkel (1954) and a degree of consolidation of 99.5% were used to estimate the drained displacement rate for the high plasticity shales. Faster displacement rates could have been used for some of the clays and silts. However, to avoid any possible rate effects, a displacement rate of 0.018 mm/min was used for all 32 specimens. After a drained residual strength condition is established at approximately 50 kPa, shearing is stopped and the normal stress is doubled. After consolidation at 100 kPa, the specimen is sheared again until a drained residual strength condition is obtained. This procedure is repeated for a number of effective normal stresses and is called a multistage test.

Fig. 1 presents shear stress-horizontal displacement relationships from a multistage ring shear test on the Altamira bentonitic tuff obtained from the Portuguese Bend landslide near Los Angeles, Calif. The bentonitic tuff sample was obtained from the slip surface at the toe of the landslide approximately 150 m east of Inspiration Point. The remolded tuff sample classifies as a clay of high plasticity, CH, according to the Unified Soil Classification System. The liquid limit, plasticity index, and clay-size fraction of the remolded bentonitic tuff sample are 98, 61, and 68%, respectively. It can be seen from Fig. 1 that during the first stage of shearing at an effective normal stress ( $\sigma_v'$ ) of 60 kPa the specimen exhibited a small peak strength. The peak strength of approximately 20 kPa was mobilized at a horizontal displacement of about 0.02 cm. The residual strength of approximately 15 kPa was reached at a horizontal displacement of approximately 2.0 cm. The small peak strength observed for an overconsolidation ratio of 12 is caused by the effectiveness of the precutting process in forming a shear surface. Since the maximum effective normal stress on the slip surface at Portuguese Bend is approximately 640 kPa, the last stage of the multistage test had to be conducted at a normal stress greater than 480 kPa. Doubling the normal stress from 480 kPa would require a normal stress of 960 kPa. However, it was decided to use only 850 kPa because it significantly exceeds the maximum effective normal stress on the slip surface of 640 kPa.

It can also be seen from Fig. 1 that the specimen underwent a vertical displacement of approximately 0.008 cm (i.e., 1.6% of the initial height) during the first stage of shear. This small vertical displacement is due to the specimen having an overconsolidation ratio of 12 and the precutting process reducing the horizontal displacement required to achieve a residual strength condition. For comparison purposes, a normally consolidated, intact, re-

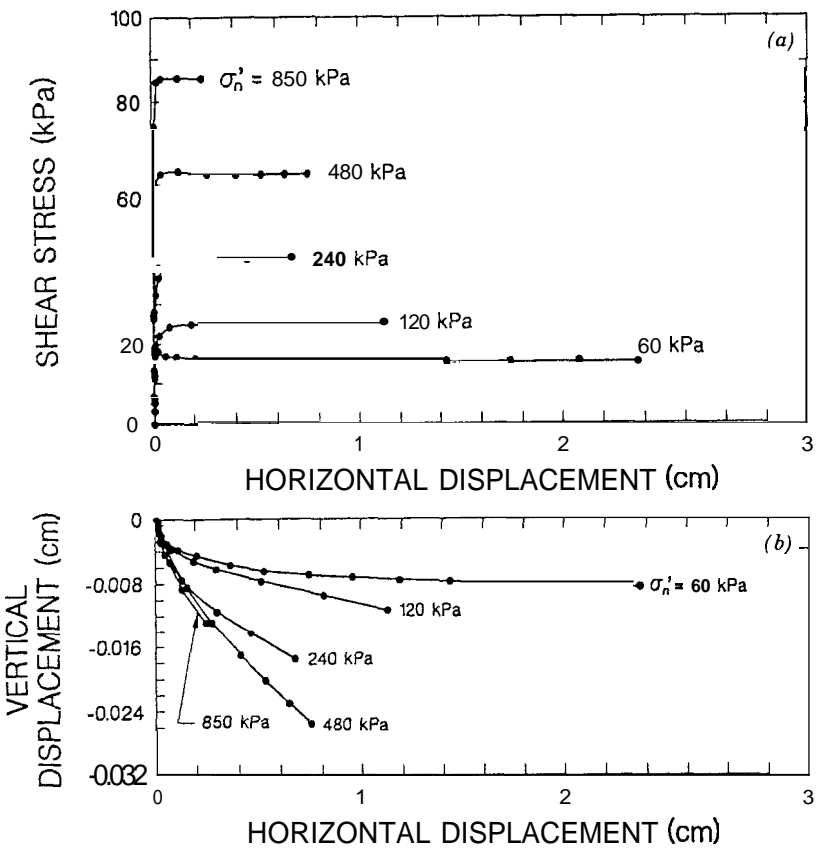


FIG. 1. Drained Multistage Ring Shear Test on Altarnira Bentonitic Tuff

molded specimen required 9.9 cm of horizontal displacement and underwent 0.043 cm of vertical displacement before achieving a residual strength condition. The second stage of this ring shear test was conducted at an effective normal stress of 120 kPa and is also shown in Fig. 1. Since a residual strength condition was reached during the first stage of the test, the specimen did not exhibit a peak strength. In addition, only approximately 1.2 cm of horizontal displacement was required to obtain a residual strength of about 26 kPa. A similar behavior was observed during the remaining three phases of the multistage test.

### NONLINEARITY OF DRAINED RESIDUAL STRENGTH ENVELOPE

Ring shear tests on 32 clays and clayshales (Table 1) were used to establish the effect of clay mineralogy on the drained residual failure envelope. Fig. 2 presents the drained residual failure envelopes for seven of the clays and clayshales tested during this study. It can be seen that the magnitude of the drained residual strength decreases with increasing liquid limit. It also appears that the drained residual strength decreases with increasing activity. The activity ( $A_v$ ) is defined as the plasticity index divided by the clay-size

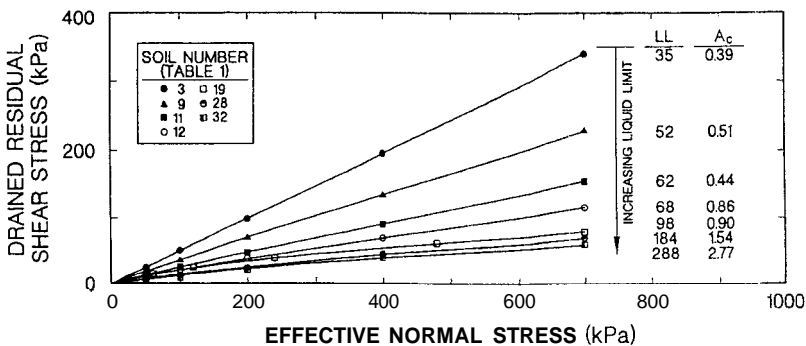


FIG. 2. Effect of Clay Mineralogy on Drained Residual Failure Envelopes

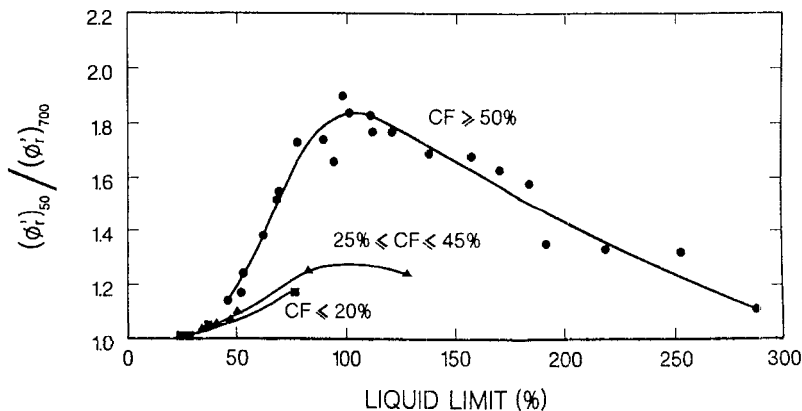


FIG. 3. Reduction in Secant Residual Friction Angle from Effective Normal Stresses of 50 kPa to 700 kPa

fraction. Both the liquid limit and activity provide an indication of clay mineralogy, and thus particle size and shape. In general, the plasticity increases as the platyness of the clay particles increases. Increasing the platyness of the particles results in a greater tendency for face-to-face interaction, and thus a lower drained residual strength.

Fig. 2 also shows that the drained residual failure envelope can be non-linear. This nonlinearity appears to be significant for cohesive soils with moderate to high liquid limit and activity. Fig. 3 presents the ratio of the secant residual friction angle at 50 kPa,  $(\phi_r)_{50}$ , and 700 kPa,  $(\phi_r)_{700}$ , for the 32 cohesive soils listed in Table 1. The secant residual friction angle corresponds to a linear failure envelope passing through the origin and the residual shear stress at a particular effective normal stress. It can be seen that the ratio of  $(\phi_r)_{50}$  to  $(\phi_r)_{700}$  is less than 1.3 for clay-size fractions (CF) less than 45%. For clay size fractions greater than 50%, the ratio of  $(\phi_r)_{50}$  to  $(\phi_r)_{700}$  reaches a maximum of 1.85 to 1.9 at a liquid limit of approximately 100 and decreases to about 1.1 at a liquid limit of 288. Therefore, it may be concluded that the nonlinearity of the residual failure envelope is significant, i.e.,  $(\phi_r)_{50}/(\phi_r)_{700}$  is greater than 1.3, for cohesive soils with a liquid limit between 60 and 220 and a clay-size fraction greater than 50%. In this

range of liquid limit and clay-size fraction, the residual friction angle undergoes a reduction of 25–45% for effective normal stresses increasing from 50 to 700 kPa.

The nonlinearity of the drained residual failure envelope can be explained in terms of particle size and platyness. For soils of low clay-size fraction (CF less than 45%), and soils with a liquid limit less than 60 and a clay-size fraction greater than 50%, the relatively rotund particles and/or stiff clay plates dominate the shear behavior. These particles are able to establish edge-to-face interaction even at the drained residual condition. Consequently, the initial contact area and the increase in contact area during shear are small under any range of effective normal stresses. This leads to an approximately linear drained residual failure envelope. A linear failure envelope also occurs in soils with high clay-size fraction (CF greater than 50%) and plasticity (LL greater than 220) but by a different mechanism. The highly flexible and platy particles of these soils establish face-to-face interaction even under low effective normal stresses. Consequently, the initial contact area is large and the increase in contact area during shear is small under any range of effective normal stress. This also results in a linear failure envelope.

Soils with a clay-size fraction greater than 50% and a liquid limit between 60 and 220 initially have a combination of edge-to-face and face-to-face interaction. At low effective normal stresses edge-to-face interactions can exist and then shearing converts some edge-to-face interactions to face-to-face. This increases the contact area during shear and decreases the measured strength until a residual value is obtained. As the effective normal stress increases, initial edge-to-face interactions are compressed to form a face-to-face orientation and increases the contact area prior to shear. As a result, the contact area at the residual condition is substantially greater at high effective normal stresses than at low effective normal stresses for this group of soils. This difference in contact area results in a nonlinear residual failure envelope.

## NEW DRAINED RESIDUAL STRENGTH CORRELATION

Fig. 4 presents a correlation of drained residual friction angle and soil index properties. at effective normal stress of 100, 400, and 700 kPa. It can be seen that there is a relationship between the secant residual friction angle and both liquid limit and clay-size fraction. The higher the liquid limit and clay-size fraction the lower the secant residual friction angle. The liquid limit appears to be a suitable indicator of clay mineralogy, and thus drained residual strength. However, clay-size fraction remains an important predictive parameter because it indicates the quantity of particles smaller than 0.002 mm. The proposed correlation differs from existing correlations because the drained residual friction angle is a function of liquid limit, clay-size fraction, and effective normal stress.

Fig. 4 also illustrates the nonlinearity of the drained residual failure envelope in terms of the decrease in secant residual friction angle with increasing effective normal stress. It confirms that the nonlinearity is significant for cohesive soils with a clay-size fraction greater than 50% and liquid limit between 60 and 220. For example, at a liquid limit of 100 and a clay-size fraction greater than 50% in Fig. 4, the secant residual friction angle decreases from 9.5° at an effective normal stress of 100 kPa to 6.2° (or 35%) at an effective normal stress of 700 kPa. For clay-size fractions less than

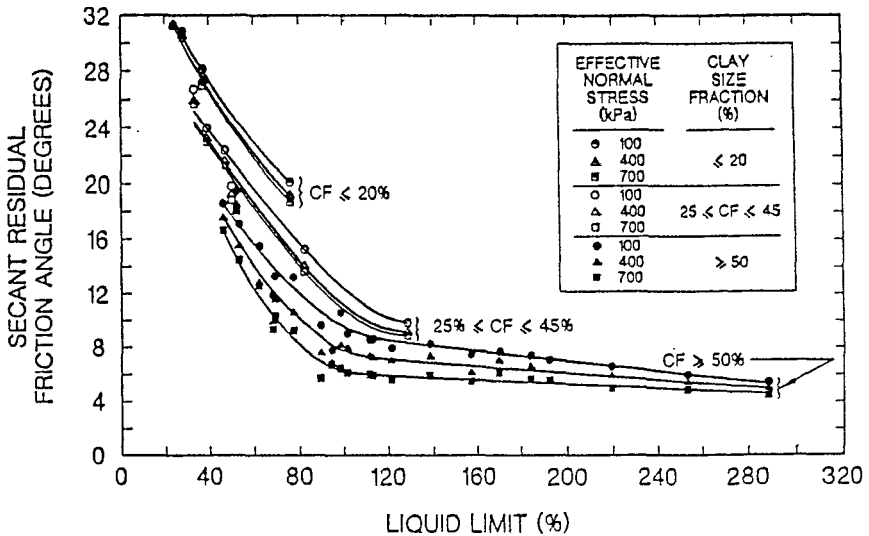


FIG. 4. Relationship between Drained Residual Friction Angle and Liquid Limit

45% and liquid limits less than 120, the reduction in secant residual friction angle from 100 to 700 kPa is less than 1–2° (Fig. 4).

The secant residual friction angle for a cohesive soil can be estimated for a particular effective normal stress using the liquid limit, clay-size fraction, and interpolation between the curves presented in Fig. 4. For stability analyses it is shown in a subsequent section that the average effective normal stress acting on the slip surface should be used to estimate the residual friction angle in Fig. 4. The effective normal stress can easily be estimated because the location of the critical slip surface is well defined by the pre-existing shear surface. Fig. 4 can also be used to estimate the nonlinear residual failure envelope by plotting the shear stress corresponding to the drained residual friction angle at effective normal stresses of 100, 400, and 700 kPa. A smooth curve can be drawn through the three points and the origin to estimate the nonlinear failure envelope. For clay-size fractions between 20% and 25% and 45% and 50%, the residual friction angle can be estimated for a particular effective normal stress by interpolation between the clay-size fraction groups.

#### EFFECT OF NONLINEAR RESIDUAL FAILURE ENVELOPE ON STABILITY ANALYSES

It is clear from the previous section that the drained residual failure envelope for cohesive soils with a liquid limit less than 120 and a clay-size fraction less than 45% can be modeled using a straight line in stability analyses. However, cohesive soils with a clay-size fraction greater than 50% and a liquid limit between 60 and 220 exhibit a residual failure envelope that is nonlinear. The effect of this nonlinearity on stability analyses was investigated using a number of field case histories. Two of these case histories are described in the following.

The Portuguese Bend landslide is a reactivated part of a 5.2 km<sup>2</sup> landslide on the south flank of the Palos Verdes Peninsula, near Los Angeles, Calif.



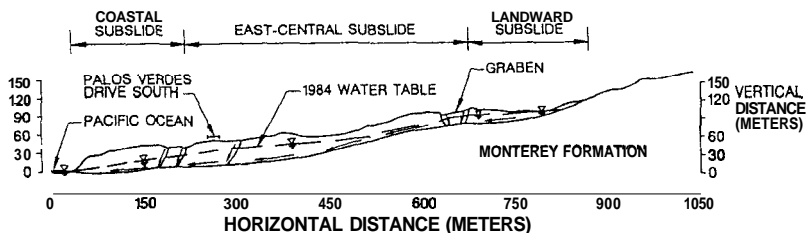


FIG. 5. Typical Cross Section through Portuguese Bend Landslide [after Ehlig (1987)]

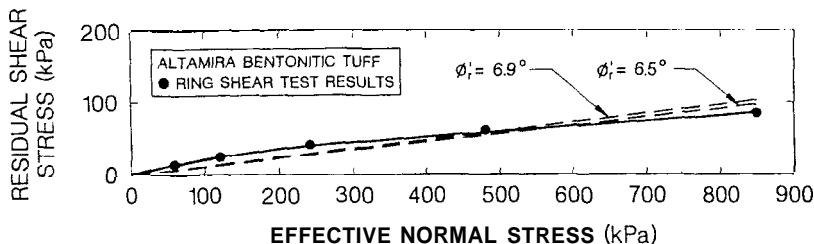


FIG. 6. Drained Residual Failure Envelope for Altamira Bentonitic Tuff

Recent movement of the landslide began in 1956 when 1.052 km<sup>2</sup> slid during a surge in subdivision development. However, the Portuguese Bend landslide has long been recognized as a large slowly moving landslide on the south slope of the Palos Verdes Hills (Woodring et al. 1946). Recent movement has continued from 1956 to 1976 at an average rate of 1 cm per day. From 1976 to 1986, the displacement rate increased to 2.5 cm per day, which is attributed to wave erosion removing slide material at the toe and an increase in ground-water levels. The slide movement appears to be controlled by the coastal subslides (Fig. 5), and field observations show that, if the coastal subslide moves, the remainder of the slide also moves (Ehlig 1992). It can be seen that the depth of the slip surface in the subslides ranges from 30 to 45 m, which corresponds to an effective normal stress of 300–640 kPa. The mean effective normal stress on the slip surface in the first subslide is estimated to be 500 kPa.

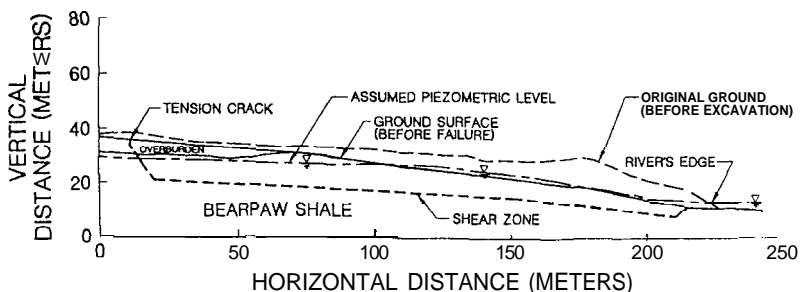
Sliding is occurring along thin bentonitic tuffaceous beds in the Altamira shale member of the middle Miocene Monterey Formation. The tuffaceous beds consist of bentonite that is predominantly calcium-montmorillonite. The liquid limit, plasticity index, and clay-size fraction of the remolded bentonitic tuff sample are 96, 61, and 68%, respectively. The slope has been moving since the initial Pleistocene landslide; as a result the shear strength of the bentonitic tuff in this area is probably at the residual value.

Fig. 6 shows the nonlinear residual failure envelope measured for the bentonitic tuff and two linear approximations of the failure envelope. A linear failure envelope passing through the origin and the test data in the effective normal stress range of 300–640 kPa yields a residual friction angle of approximately 6.5°. Another linear failure envelope inclined at 6.9° corresponds to the secant residual friction angle estimated from Fig. 4 using the average effective normal stress of 500 kPa.

Table 2 presents the factors of safety calculated using the cross section

**TABLE 2. Calculated Factors of Safety for Portuguese Bend Landslide**

Effective cohesion (kPa) (1)	Effective friction angle (degrees) (2)	Factor of safety (3)
nonlinear	nonlinear	1.02
0	6.5	1.00
0	6.9	1.04



**FIG. 7. Cross Section through Gardiner Dam Slide [after Jasper and Peters (1979)]**

in Fig. 5, Spencer's (1967) stability method, and the three failure envelopes in Fig. 6. The nonlinear residual failure envelope was modeled using 19 data points in UTEXAS2 (Wright 1986). The average moist unit weight of the slide mass was measured to be 17.5 kNm<sup>3</sup>.

It can be seen that the three failure envelopes yield factors of safety that are in good agreement with field observations. Each envelope provides the stability analysis with the residual strength corresponding to typical values of effective normal stress acting on the slip surface. It can be seen in Fig. 6 that other envelopes could be drawn through the data points, many of which would not provide good agreement with field observations. In conclusion, test data and correlations must evaluate the residual strength over the appropriate range of effective normal stress. This can be accomplished by modeling the entire nonlinear envelope in a stability analysis or estimating the residual friction angle (from test data or Fig. 4) that corresponds to the average effective normal stress on the critical slip surface.

The second case history involves a landslide that occurred in an excavated slope near the tunnel inlet area at Gardiner Dam (Jasper and Peters 1979). Gardiner Dam is located on the South Saskatchewan River, in western Canada, and is underlain by the Bearpaw Formation. The Bearpaw Formation at this location consists of two sandstone units and an intervening clay shale unit, which contains bentonite or bentonitic zones. The shale is a highly overconsolidated marine clay deposited in late Cretaceous time (Jasper and Peters 1979; Peterson et al. 1960). The greenish-gray shale is noncalcareous with a liquid limit, plasticity index, and clay-size fraction of 128, 101, and 43%, respectively. The remolded shale classifies as a clayey-sand, SC, according to the Unified Soil Classification System. The shale contained preexisting shear surfaces that led to a number of slides during trench excavations and abutment slope trimming throughout construction of Gardiner Dam. As a result, major design modifications consisting of extensive upstream and downstream slope flattening (12 horizontal to 1 vertical instead of 8 horizontal to 1 vertical) and a 250-m downstream toe

berm with a slope of 85 horizontal to 1 vertical were required to compensate for the preexisting shear surfaces in the Bearpaw shale (Peck 1988). The average unit weight of the Bearpaw shale and overburden (Fig. 7) were measured to be  $19.0 \text{ kN/m}^3$  and  $18.7 \text{ kN/m}^3$ , respectively (Ringheim 1964). Fig. 8 shows the slightly nonlinear drained residual failure envelope obtained from a multistage ring shear test on Bearpaw shale. The measured residual failure envelope (Fig. 8) for the Bearpaw shale at Gardiner Dam yielded a factor of safety of 1.01 for the cross section shown in Fig. 7. The slightly nonlinear failure envelope was modeled using 19 data points in UTEXAS2.

The average effective normal stress on the slip surface was estimated to be 95 kPa. Fig. 4, the liquid limit, clay-size fraction, and average effective normal stress on the slip surface of 95 kPa were used to estimate a residual friction angle of  $9.8^\circ$ . The estimated residual friction angle of  $9.8^\circ$  yielded a factor of safety of 1.02. Fig. 8 provides a comparison of the measured and estimated residual failure envelopes for the Bearpaw shale. It can be seen that the estimated residual friction angle of  $9.8^\circ$  is in excellent agreement with the measured envelope at effective normal stresses less than 200 kPa. Therefore, the estimated residual friction angle is in excellent agreement with field observations because the average effective normal stress on the slip surface is 95 kPa. However, if the average effective normal stress on the base of the slip surface was higher, for example 400 kPa, the proposed correlation would have predicted a residual friction angle of  $8.8^\circ$ , which is in good agreement with the measured failure envelope near 400 kPa (Fig. 8). Therefore, the proposed correlation in Fig. 4 can provide an excellent estimate of the nonlinear residual failure envelope, and thus field observations, by using a residual friction angle that corresponds to the average effective normal stress on the critical slip surface.

### COMPARISON OF EMPIRICAL CORRELATIONS FOR DRAINED RESIDUAL STRENGTH

To illustrate the importance of using both liquid limit and clay size fraction together in estimating the drained residual friction angle, the proposed and existing correlations are compared using the Gardiner Dam and Portuguese Bend field case histories. The trend line or average residual friction angle was used from the existing correlations except for Mesri and Cepeda-Diaz (1986) and Voight (1973), where the data point corresponding to Bearpaw shale from Gardiner Dam was used. Table 3 provides a comparison of the proposed and existing empirical correlations for drained residual strength. It can be seen from Table 3 that most of the previous residual strength correlations based on clay-size fraction overestimate the factor of safety for

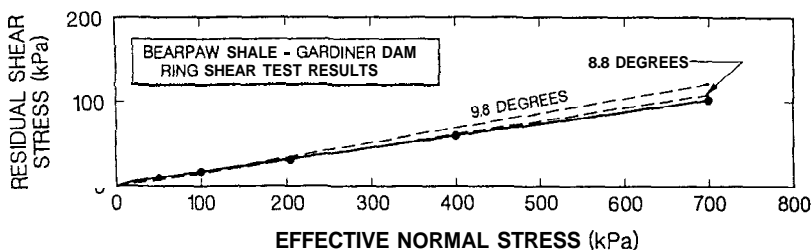


FIG. 8. Drained Residual Failure Envelope for Bearpaw Shale from Saskatchewan, Canada

**TABLE 3. Comparison of Empirical Correlations for Drained Residual Strength Using Field Case Histories**

Soil index property (1)	Reference (2)	Gardiner Dam (LL = 128; FI = 101; CF = 43)		Portuguese Bend (LL = 98; PI = 61; CF = 68)	
		Residual friction angle (3)	Factor of safety (4)	Residual friction angle (5)	Factor of safety (6)
Liquid limit and clay fraction	Current study	9.8	1.02	6.9	1.04
Clay fraction	Skernpton (1964)	18.0	1.91	12.3	1.67
	Borowicka (1965)	7.5	0.77	7.5	1.12
	Binnie et al. (1967)	15.2	1.61	11.5	1.58
	Blondeau and Josseume (1976)	12.6	1.31	7.0	1.06
	Lupini et al. (1981)	13.4	1.41	4.9	0.81
	Skempton (1985)	— <sup>a</sup>	— <sup>a</sup>	11.1	1.53
	Collotta et al. (1989)	11.8	1.23	7.8	1.15
Plasticity index	Fleischer (1972)	9.1	0.94	9.1	1.30
	Voight (1973)	6.3	0.65	9.8	1.38
	Kanji (1974)	6.0	0.61	7.5	1.12
	Bucher (1975)	— <sup>a</sup>	— <sup>a</sup>	— <sup>a</sup>	— <sup>a</sup>
	Mitchell (1976)	10.9	1.13	11.6	1.59
	Seyček (1978)	7.8	0.81	9.6	1.36
	Vaughan et al. (1978)	— <sup>a</sup>	— <sup>a</sup>	— <sup>a</sup>	— <sup>a</sup>
	Lambe (1985)	— <sup>a</sup>	— <sup>a</sup>	— <sup>a</sup>	— <sup>a</sup>
	Clemente (1992)	11.6	1.21	11.6	1.59
Liquid limit	Haefeli (1951)	— <sup>a</sup>	— <sup>a</sup>	— <sup>a</sup>	—
	Mitchell (1976)	13.0	1.36	13.0	1.75
	Mesri and Cepeda (1986)	9.4	0.97	8.0	1.18

<sup>a</sup>Not applicable

the Gardiner Dam case history. The Bearpaw shale has a high liquid limit (128) but a relatively low clay-size fraction (43%). The high liquid limit results in a measured secant residual friction angle at an effective normal stress equal to 700 kPa of approximately 8.5" (Fig. 8). However, existing correlations based on clay-size fraction predict a residual friction angle of approximately 12°–18°. It was anticipated that existing correlations would not provide an accurate estimate of this residual friction angle, because of the high liquid limit (128) and low clay-size fraction (43%), of the Bearpaw shale. Typically a high liquid limit corresponds to a high clay-size fraction. However, this relation need not be general, as is illustrated by a number of the clays and clayshales tested during this study. It should be noted that the correlation proposed by Borowicka (1965) yielded a conservative estimate of the residual friction angle (7.5") for the Bearpaw shale at Gardiner Dam. The correlation presented by Skempton (1985) is also based on clay-

size fraction but it is limited to soils with an activity between 0.5 and 0.9, and thus is not applicable to Bearpaw shale, which has an activity of 2.35.

Existing correlations based on clay-size fraction produced conflicting factors of safety for the Portuguese Bend case history (Table 3). Most of these correlations overestimated the Portuguese Bend factor of safety, while the correlation proposed by Lupini et al. (1981) underestimated the factor of safety. The correlation proposed by Blondeau and Josseume (1976) provided the best agreement with Portuguese Bend field observations. In summary, existing correlations based on only clay-size fraction tend to overestimate the drained residual friction angle. It is imperative that drained residual strength correlations incorporate both liquid limit and clay-size fraction to provide an accurate estimate of clay mineralogy and the quantity of clay-size particles, respectively. In addition, neglecting the nonlinearity of the residual failure envelope, i.e., the average effective normal stress acting on the slip surface, probably aided the poor estimate of the factor of safety for the Portuguese Bend case history.

Existing correlations that utilize plasticity index or liquid limit also yielded conflicting factors of safety for the Gardiner Dam case history. Four of the correlations underestimated the residual friction angle, and thus the factor of safety, for the Gardiner Dam case history. However, Mitchell (1976) and Clemente (1992) overestimated the residual fraction angle, and Fleischer (1972) provided the best agreement with field observations. Mesri and Cepeda-Diaz (1986) data point for the Bearpaw shale at Gardiner Dam corresponds to a residual friction angle of 9.4° and a factor of safety equal to 0.97. All existing correlations based on plasticity index or liquid limit overestimated the residual friction angle, and thus the factor of safety, for the Portuguese Bend landslide. This is caused by the Altamira bentonitic tuff exhibiting a plasticity index of 61 and a clay-size fraction of 68.

In conclusion, the drained residual strength is controlled by the type of clay mineral and quantity of clay-size particles. The liquid limit and clay-size fraction in general provide an accurate estimate of the type of clay mineral and the quantity of clay-size particles, respectively. Therefore, existing correlations based on either clay-size fraction or clay plasticity do not provide a consistent estimate of the drained residual friction angle. In addition, the residual failure envelope can be approximated by a straight line for cohesive soils that have a clay size fraction less than 45%. For cohesive soils with clay size fraction greater than 50% and a liquid limit between 60 and 220, the nonlinearity of the drained residual failure envelope is significant. Existing drained residual strength correlations do not provide an estimate of this nonlinearity. Since the residual strength is usually small, small changes in the residual friction angle result in significant changes in the calculated factor of safety. Therefore, the stress-dependent nature of the residual strength is important in slope stability analyses. A new correlation is proposed to overcome the limitations of existing correlations and provide better agreement with field case histories.

## CONCLUSIONS

The following conclusions are based on the results of torsional ring shear tests on 32 clays and clayshales.

1. The magnitude of the drained residual strength is controlled by the type of clay mineral and quantity of clay-size particles.

2. The liquid limit provides an indication of clay mineralogy and the clay-size fraction indicates the quantity of particles smaller than 0.002 mm. Therefore, both the liquid limit and clay-size fraction should be used to estimate the drained residual friction angle.

3. The drained residual strength failure envelope is nonlinear. The nonlinearity is significant for cohesive soils with a clay size fraction greater than 50% and a liquid limit between 60 and 220. This nonlinearity should be incorporated into stability analyses.

4. A new drained residual strength correlation is described that is a function of the liquid limit, clay-size fraction, and effective normal stress. The correlation can be used to estimate the entire nonlinear residual failure envelope or a secant residual friction angle that corresponds to the average effective normal stress on the slip surface.

5. It is recommended that the nonlinear residual failure envelope or a secant residual friction angle corresponding to the average effective normal stress on the slip surface be used in a stability analysis to model the effective stress dependent behavior of the residual strength.

### ACKNOWLEDGMENTS

This study was performed as a part of National Science Foundation Grant BCS-91-96074. The support of this agency is gratefully acknowledged. Poul V. Lade and Stephen M. Watry of the University of California at Los Angeles provided the sample of the Altamira bentonitic shale. Serge Leroueil of Laval University provided the sample of Brown London Clay. E. Karl Sauer of the University of Saskatchewan provided the sample of the Lea Park bentonitic shale. The writers acknowledge G. Mesri for his many valuable suggestions during this study.

### APPENDIX. REFERENCES

- Anayi, J. T., Boyce, J. R., and Rodgers, C. D. (1988). "Comparison of alternative methods of measuring the residual strength of a clay." *Transp. Res. Record 1192*, Transportation Research Board (TRB), Washington, D.C.
- Anayi, J. T., Boyce, J. R., and Rodgers, C. D. F. (1989). "Modified ring shear apparatus." *ASTM Geotech. J.*, 12(2), 171-173.
- Binnie, M. A., Clark, J. F. F., and Skempton, A. W. (1967). "The effect of discontinuities in clay bedrock on the design of dams in the Mangle project." *Trans. 9th Int. Congress on Large Dams*, International Commission on Large Dams (ICOLD), Paris, France, Vol. 1, 165-183.
- Blondeau, F., and Josseume, H. (1976). "Mesure de la résistance au cisaillement résiduelle en laboratoire." *Bulletin de Liaison des Laboratoires des Ponts et Chaussées; Stabilité de talus I; versants naturels*, Paris, France (numéro spécial II), 90-106 (in French).
- Borowicka, H. (1965). "The influence of the colloidal content on the shear strength of clay." *Proc., 6th Int. Conf. Soil Mech. and Found. Engrg.*, Montreal, Canada, Vol. 1, 175-178.
- Bromhead, E. N. (1979). "A simple ring shear apparatus." *Ground Engrg.*, 12(5), 40-44.
- Bromhead, E. N., and Curtis, R. D. (1983). "A comparison of alternative methods of measuring the residual strength of London clay." *Ground Engrg.*, 16(4), 39-41.
- Bucher, F. (1975). "Die Restscherfestigkeit natürlicher Böden, ihre Einflussgrößen und Beziehungen als Ergebnis experimenteller Untersuchungen." *Rep. No. 103*, Institutes für Grundbau und Bodenmechanik Eidgenössische Technische Hochschule, Zürich, Switzerland (in German).

- Clemente, J. L. (1992). "Strength parameters for cut slope stability in 'Marine' Sediments." *Proc., ASCE Specialty Conf. on Stability and Performance of Slopes and Embankments — II*. ASCE, New York, N.Y., Vol. 1, 865–875.
- Collotta, T., Cantoni, R., Pavesi, U., Ruberl, E., and Moretti, P. C. (1989). "A correlation between residual friction angle, gradation and the index properties of cohesive soils." *Géotechnique*, London, England, 39(2), 343–346.
- Ehlig, P. L. (1987). "The Portuguese Bend landslide stabilization project." *Geology of Palos Verdes Peninsula and San Pedro Bay*. P. J. Fishcher, ed., Society of Economic Paleontologists and Mineralogists and American Association of Petroleum Geologists, Los Angeles, Calif., Part 2, 17–24.
- Ehlig, P. L. (1992). "Evolution, mechanics and mitigation of the Portuguese Bend landslide, Palos Verdes Peninsula, California." *Engineering geology practice in southern California*, B. W. Pipkin and R. J. Proctor, eds., Star Publishing Co., Belmont, Calif., pp. 531–553.
- Fleischer, S. (1972). "Scherbruch- und Schergleitfestigkeit von Bindigen Erdstoffen." *Neue Bergbautechnik*, Freiburg, Germany, 2(2), 98–99 (in German).
- Gibson, R. E., and Henkel, D. J. (1954). "Influence of duration of tests at constant rate of strain on measured 'Drained' strength." *Géotechnique*, London, England, 4(1), 6–15.
- Haefeli, R. (1951). "Investigation and measurements of the shear strength of saturated cohesive soils." *Géotechnique*, London, England, 2(3), 186–207.
- Hawkins, A. B., and Privett, K. D. (1984). "Residual strength: Does BS 5930 help or hinder?" *Proc., 20th Conf. of the Engrg. Group Geological Soc., Site Investigation Practice: Assessing BS 5390*, The Geological Society, London, England, Vol. 1, 274–280.
- Hawkins, A. B., and Privett, K. D. (1985). "Measurement and use of residual shear strength of cohesive soils." *Ground Engrg.*, 18(8), 22–29.
- Jaspar, J. L., and Peters, N. (1979). "Foundation performance of Gardiner Dam." *Can. Geotech. J.*, Vol. 16, 758–788.
- Kanji, M. A. (1974). "The relationship between drained friction angles and Atterberg limits of natural soils." *Géotechnique*, London, England, 24(4), 671–674.
- Kenney, T. C. (1967). "The influence of mineral composition on the residual strength of natural soils." *Proc., Geotech. Conf., Vol. 1*, Norwegian Geotechnical Institute, Oslo, Norway, 123–129.
- Lambe, T. W. (1985). "Amuay landslides." *Proc., XI Int. Conf. Soil Mech. and Found. Engrg.* A. A. Balkema Publishing Co., Rotherdam, The Netherlands, 137–158.
- Lupini, J. F., Skinner, A. E., and Vaughan, P. R. (1981). "The drained residual strength of cohesive soils." *Géotechnique*, London, England, 31(2), 181–213.
- Maksimovic, M. (1989). "On the residual shearing strength of clays." *Géotechnique*, London, England, 39(2), 347–351.
- Mesri, G., and Cepeda-Diaz, A. F. (1986). "Residual shear strength of clays and shales." *Géotechnique*, London, England, 36(2), 269–274.
- Mitchell, J. K. (1976). *Fundamentals of soil behavior*. John Wiley and Sons, New York, N.Y.
- Peck, R. B. (1988). "The place of stability calculations in evaluating the safety of existing embankment dams." *Civ. Engrg. Practice*, Boston Society of Civil Engineers, (Fall), 67–80.
- Peterson, R., Jaspar, J. L., Rirard, P. J., and Iverson, N. L. (1960). "Limitations of laboratory shear strength in evaluating stability of highly plastic clay's." *Proc., Conf. on Shear Strength of Cohesive Clays*, ASCE, New York, N.Y., 765–791.
- Ringheim, A. S. (1964). "Experiences with the Bearpaw shale at the South Saskatchewan River Dam." *Proc., 8th Int. Congress on Large Dams, Vol. 1*, International Commission on Large Dams, Paris, France, 529–550.
- Seyček, J. (1978). "Residual shear strength of soils." *Bull. Int. Assoc. Engrg. Geologists*, Germany, Vol. 17, 73–75.
- Skempton, A. W. (1964). "Long-term stability of clay slopes." *Géotechnique*, London, England, 14(2), 75–101.

- Skernpton, A. W. (1985). "Residual strength of clays in landslides, folded strata and the laboratory." *Geotechnique*, London, England, 35(1), 3-18.
- Spencer, E. (1967). "A method of analysis of the stability of embankments assuming parallel inter-slice forces." *Geotechnique*, London, England, 17(1), 11-26.
- Stark, T. D., and Eid, H. T. (1993). "Modified Bromhead ring shear apparatus." *ASTM Geotech. J.*, 16(1), 100-107.
- Vaughan, P. R., Hight, D. W., Sodha, V. G., and Walbancke, H. J. (1978). "Factors controlling the stability of clay fills in Britain." *Clay fills*, Institution of Civil Engineers (ICE), London, England, 203-217.
- Voight, B. (1973). "Correlation between Atterberg plasticity limits and residual shear strength of natural soils." *Geotechnique*, London, England, 23(2), 265-267.
- Woodring, W. P., Bramlette, M. N., and Kew, W. S. W. (1946). "Geology and paleontology of Palos Verdes Hills, California." *U.S. Geological Survey Paper No. 207*, U.S. Geological Survey, Washington, D.C.
- Wright, S. G. (1986). "UTEXAS2: a computer program for slope stability calculations." *Geotechnical Engineering Software GS86-1*, Department of Civil Engineering, University of Texas, Austin, Tex.